

ScholarWorks@GSU

Investigating the Synergistic effect of Leucine-Metformin-Sildenafil on Nonalcoholic Steatohepatitis

Authors	Fu, Lizhi
Citation	Fu, Lizhi. (2015). Investigating the Synergistic effect of Leucine-Metformin-Sildenafil on Nonalcoholic Steatohepatitis. Georgia State University. https://doi.org/10.57709/7443898
DOI	https://doi.org/10.57709/7443898
Download date	2026-05-20 04:09:59
Link to Item	https://hdl.handle.net/20.500.14694/2317

INVESTIGATING THE SYNERGISTIC EFFECT OF LEUCINE-METFORMIN-SILDENAFIL ON NONALCOHOLIC STEATOHEPATITIS

By

LIZHI FU

Under the Direction of HANG SHI

ABSTRACT

Nonalcoholic steatohepatitis (NASH) is a highly prevalent liver disease in the world. About 15% to 25% of patients with NASH may progress to cirrhosis and hepatocellular carcinoma. However, there remains no U.S. Food and Drug Administration (FDA)-approved therapy for NASH. Our previous studies indicate that the combination of leucine and metformin or leucine and icariin, a phosphodiesterase type 5 inhibitor (PDE5i), improved nonalcoholic fatty liver disease (NAFLD) in Diet-induced Obesity (DIO) mice. Here we aim to evaluate the synergistic effect of leucine, metformin and sildenafil combination (Leu-Met-Sil) on NASH in Atherosclerosis diet-induced mouse model. Our data show that the Leu-Met-Sil combination significantly suppressed hepatic steatosis and fibrosis. This was associated with reduced alanine aminotransferase (ALT) levels in circulation. The Leu-Met-Sil combination also decreased inflammation and increased fatty acid oxidation in liver, which may contribute to the beneficial effects of the treatment on the NASH phenotype. We conclude that Leu-Met-Sil combination could be a novel therapy for the treatment of NASH.

INDEX WORDS: NASH, Leucine-Metformin-Sildenafil, PDE5i and Therapy

INVESTIGATING THE SYNERGISTIC EFFECT OF LEUCINE-METFORMIN-
SILDENAFIL ON NONALCOHOLIC STEATOHEPATITIS

By

LIZHI FU

A Thesis Submitted in Partial Fulfillment of the Requirements for the Degree of

Master of Science

In the College of Arts and Sciences

Georgia State University

2015

Copyright by
Lizhi Fu
2015

INVESTIGATING THE SYNERGISTIC EFFECT OF LEUCINE-METFORMIN-
SILDENAFIL ON NONALCOHOLIC STEATOHEPATITIS

By

LIZHI FU

Committee Chair: Hang Shi

Committee: Hang Shi

Bingzhong Xue

Andrew Gewirtz

Electronic Version Approved:

Office of Graduate Studies

College of Arts and Sciences

Georgia State University

July 2015

DEDICATION

To my parents and my brother and sister, who always support me and give me good conditions to live and learn.

To my wife Fenfen, who always trust me and encourage me.

ACKNOWLEDGEMENTS

The first of my acknowledgement must go to my mentor Dr. Hang Shi. Thanks for your instructions on my project so that I can learn how to handle a small project by myself. Thanks for pushing me hard on my work so that I can publish two papers as first author in your lab. Thanks for your instruction and help in my life. I need to say: “You are a good mentor.”

I would like to express my appreciation to my committee members Dr. Xue and Dr. Gewirtz. Thanks for your time, your advices and comments on my research and writing.

I would also show my thanks to my friends in my lab. Thanks to Dr. Qiang Cao and Dr. Xin Cui for all your help during the whole master period. Thanks to Emily Bruggeman for all the help on my speaking and writing. Thanks to Xiaosong Yang, Anubama Rajan, Yiishyuan Chen, Lin Zha, Rui Wu, Jia Jing, Shuping Kou for all your help in the lab.

I will give my last thanks to my wife Fenfen. We came here together. Thanks for her tolerance of my bad temper and thanks for her encouragement and support for what I want to do.

Thank you all again!

TABLE OF CONTENTS

ACKNOWLEDGEMENTS	v
LIST OF TABLES	viii
LIST OF FIGURES	ix
1. INTRODUCTION.....	1
2 MATERIALS AND METHODS	5
2.1. Animal Model	5
2.2. Serum Biochemistry	6
2.3. Quantitative Real-Time PCR	6
2.4. Tissue Preparation and Historical Examination	7
2.5. Hepatic Lipid Analysis.....	8
2.6. Western Blot	8
2.7. Statistical Analysis.....	9
3. RESULTS	9
3.1. Leu-Met-Sil combination did not change body weight but decreased liver weight.	9
3.2. Leu-Met-Sil combination reduced ALT levels in serum.....	11
3.3. Leu-Met-Sil combination reduced liver steatosis and lipid accumulation... ..	12
3.4. Leu-Met-Sil combination decreased liver fibrosis.....	13
3.5. Leu-Met-Sil combination decreased hepatic inflammation.	16

3.6. Leu-Met-Sil combination decreased liver macrophage infiltration.	17
3.7. Leu-Met-Sil combination increased the expression of genes involved in fatty acid oxidation in liver.....	18
3.8. Leu-Met-Sil combination did not change hepatic AMPK signaling.....	19
4 DISCUSSION AND CONCLUSION	20
REFERENCES.....	23
APPENDICES	27
Appendix A	27
<i>Appendix A.1.....</i>	<i>27</i>
<i>Appendix A.2.....</i>	<i>27</i>
Appendix B	27
Appendix C	27

LIST OF TABLES

Table 1 The Composition of Diets.....	6
Table 2 RT-PCR probes ID and sequences	7

LIST OF FIGURES

Figure 1 Overall hypothesis.....	4
Figure 2 Leu-Met-Sil combination did not change body weight but decreased liver weight.....	9
Figure 3 Leu-Met-Sil combination reduced ALT levels in serum.....	12
Figure 4 Leu-Met-Sil combination reduced liver steatosis.....	13
Figure 5 Leu-Met-Sil combination decreased liver fibrogenesis gene expression.....	14
Figure 6 Leu-Met-Sil combination reduced liver fibrosis.....	15
Figure 7 Leu-Met-Sil combination decreased liver proinflammatory gene expression and serum CRP levels.....	16
Figure 8 Leu-Met-Sil combination decreased liver macrophage infiltration.....	17
Figure 9. Leu-Met-Sil combination increased the expression of genes involved in hepatic fatty acid oxidation.....	18
Figure 10 Leu-Met-Sil combination did not change hepatic AMPK signaling.....	19

1. INTRODUCTION

Nonalcoholic steatohepatitis (NASH) and nonalcoholic fatty liver disease (NAFLD) are highly prevalent liver diseases. Approximately 25% of the American adult population currently has NAFLD. Furthermore, 20-30% of NAFLD patients will develop into NASH that may progress to cirrhosis, end-stage liver disease, and hepatocellular carcinoma^{1 2}. Patients with NASH have an increased risk of complications after surgery, but such abnormal data had been ignored for a long time. Recently, NAFLD was found to be a cause of primary dysfunction after liver transplantation. To date, livers with severe steatosis (more than 60% of liver cells with hepatocyte ballooning) are universally rejected for liver transplantation, and there are concerns about survival rate after transplantation with moderate steatosis (30% to 60% of hepatocytes with fat droplets).

The prevalence of NASH as a cause of severe liver disease is expected to increase in the western countries in the future. Fatty liver is commonly found in patients with type 2 diabetes and obesity, and a great concern for the world is the rapidly growing prevalence of these diseases in the United States and Europe countries. Recent surveys suggest that people with type 2 diabetes will increase dramatically in the next century. It is estimated that 29 million people will be diagnosed with type 2 diabetes by 2050 in United States³. About 50% of the increase can be attributed to the increasing age of the population, and more extensive obesity in demographic composition account for the other half. Obesity is also increasing as a worldwide epidemical problems even in developing countries⁴. Based on this information, it is expected that an even larger population will be at risk of developing NASH in the near future.

Current approaches to NASH treatment have been largely unsuccessful and primarily focus on the lifestyle change. There is no U.S. Food and Drug Administration (FDA)-approved therapy for NASH⁵. Thus, our study aims to find a novel pharmacological treatment for NASH.

SIRT1 and Adenosine Monophosphate (AMP)-Activated Protein Kinase (AMPK) regulate energy metabolism through sensing Nicotinamide Adenine Dinucleotide (NAD⁺) and AMP levels⁶⁻⁹, respectively. Due to their mutual activation, AMPK and SIRT1 are activated by common activators, and produce overlapping outcomes through stimulating peroxisome proliferator-activated receptor γ co-activator α (PGC1 α) to regulate mitochondrial biogenesis and energy expenditure.^{10, 11} The SIRT1–AMPK axis is suppressed in replete energy states such as obesity and diabetes. Activation of this axis improves insulin resistance, and lipid metabolism.¹²⁻¹⁴

Branched-chain amino acid L-leucine activates SIRT1¹⁵⁻¹⁸, which subsequently activates AMPK through SIRT1–AMPK axis^{13, 14, 15}. This results in significant synergy of leucine with polyphenols, a SIRT 1 activator, and with metformin, leading to significant increases in efficacy of treatment.¹⁵⁻¹⁹

Nitric oxide (NO) levels also response to energy status and are increased during caloric restriction. Increased NO stimulates SIRT1 activity^{20, 21}. SIRT1 reciprocally increases NO levels via deacetylation (Lys 496; Lys 506) of endothelial nitric oxide synthase (eNOS)^{22, 23}. AMPK plays a similar role via phosphorylating eNOS (Ser 1177)^{24, 25}. Thus, SIRT1, AMPK, and NO form a cross-talk energy-sensing network. The classically-established NO action mode is stimulating soluble NO-sensitive guanylyl cyclase (GC) to increase cGMP, and initiating subsequent physiological changes primarily via cGMP-dependent protein kinases (PKGs)²⁶. cGMP signaling termination depends on dependent upon phosphodiesterase (PDE)-mediated hydrolysis. Comparable effects are obtained by inhibiting cGMP-specific PDE5 using specific inhibitors, such as

sildenafil and icariin^{26, 27}. However, these PDE5i also activate eNOS²⁸⁻³⁰ and may increase SIRT1 activity and improve lipid metabolism and insulin signaling.^{28,31, 32}

Our published data indicate that L-leucine and PDE5i combination not only promoted insulin sensitivity but also improved NAFLD in Diet-induced Obesity (DIO) mice³³.

Metformin is considered as the first-line drug for treating type 2 diabetes. It exhibits an excellent safety profile and does not promote weight gain³⁴. However, its therapeutic function is often limited by dose-related gastrointestinal adverse effects (especially at the full therapeutic dose of 1500 to 2000 mg/day). This leads to dose reduction and/or compliance issues in 30% of patients and drug discontinuation in up to 10% of patients³⁵. Moreover, metformin monotherapy often fails to achieve optimal glycemic control due to inter-individual variability in response to drug initiation and maintenance.³⁶

Metformin lowers blood glucose mainly through suppressing hepatic glucose production and increasing peripheral glucose disposal³⁷⁻³⁹. Most of these effects depend on AMPK/Sirt1 pathway activation. Metformin inhibits mitochondrial respiratory chain complex I⁴⁰ and AMP-deaminase⁴¹. These result in elevated AMPK activity. AMPK activation increases NAD⁺/NADH ratio, which leads to increased SIRT1 activity⁴².

Type 2 diabetes is characterized by insulin resistance, which leads to impaired glucose and lipid metabolism in muscle, adipose tissue, and liver. AMPK and Sirt1 are two key regulators of energy status. They are bidirectional and cross-activated, and they produce similar metabolic effects^{43, 44}. Decreased activity of the AMPK/Sirt1 axis is associated with obesity, insulin resistance, and diabetes. However, activating either one prevents and improves hyperglycemia and insulin resistance.^{12-14, 45}

Our previous studies indicate that the combination of leucine with a low dose of metformin not only promoted insulin sensitivity but also improved NAFLD in Diet-induced Obesity (DIO) mice¹⁹. Similarly, we found that leucine and PDE5 inhibitor combination had the same effect on NAFLD³³. The present study was designed to more comprehensively evaluate the efficacy of synergistic effect of leucine-metformin-PDE5i (sildenafil) on NASH (**Figure 1**).

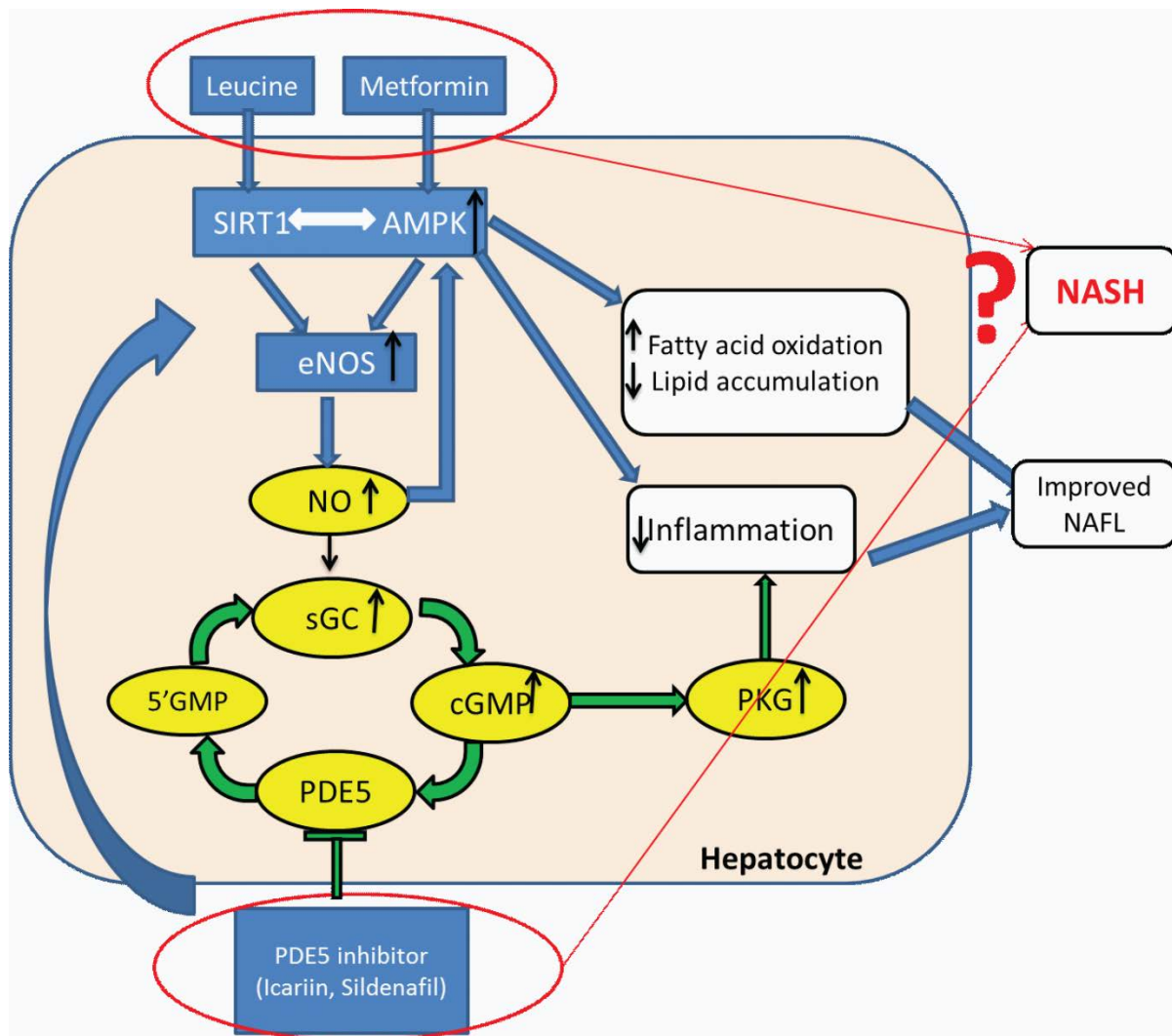


Figure 1. Overall hypothesis

Figure 1 Overall hypothesis.

2 MATERIALS AND METHODS

2.1. Animal Model

Eighty 6-week old male C57BL/6 mice from Jackson Lab were put on either low-fat (LF) diet or HF/ATH (atherogenesis)(containing 1.25% cholesterol, 0.5% cholate by weight and 60% calories as saturated fat (lard)) for 4 weeks to induce NASH. Based on the ALT levels measured in serum of NASH model, mice were then be assigned to receive either the LF or the HF/ATH diet with or without different leucine-metformin-sildenafil (Leu-Met-Sil) combinations indicated in the table (**Table.1**) for an additional 5 weeks

Animals were housed in polypropylene cages at room temperature of 22° C with a 12 h light/dark cycle. The animals had free access to water and assigned food throughout the experiment. Body weight was measured weekly. After 5-week treatment, all of the animals were euthanized with CO₂ and dissected. Blood and tissues were collected for further experiments. This study and all animal procedures were conducted under the auspices of an Institutional Animal Care and Use Committee-approved protocol of the Georgia State University.

Table 1 The Composition of Diets

Table 1. The Composition of Diets							
Composition	LF (LF)	HF/ATH (HC)	HF/ATH+Sil (Sil)	HF/ATH+Leu+Sil (Leu-sil)	HF/ATH Leu+Met (Leu-Met)	HF/ATH+Sil+Met (Met-Sil)	HF/ATH+Leu+Met+Sil (Leu-Met-Sil)
Calories from fat	10%	60%	60%	60%	60%	60%	60%
Cholesterol	N.	1.25%	1.25%	1.25%	1.25%	1.25%	1.25%
Cholate	N.	0.5%	0.5%	0.5%	0.5%	0.5%	0.5%
Leu	N.	N.	N.	24 g/kg diet	24 g/kg diet	N.	24 g/kg diet
Met	N.	N.	N.	N.	0.25 g/kg diet	0.25 g/kg diet	0.25 g/kg diet
Sil	N.	N.	25mg/kg diet	25mg/kg diet	N.	25mg/kg diet	25mg/kg diet
Abbreviations: LF, Regular chow diet; HF/ATH, High fat/atherogenic diet; Leu, L-Leucine; Met, Metformin; Sil, Sildenafil;							

2.2.Serum Biochemistry

Blood was collected via tail vein, and Total Cholesterol (TC) and Triglyceride (TG) were measured using Kit from Wako Pure Chemical Industries (Osaka, Japan). Serum C-reactive protein (CRP) levels were measured in fed mice using a mouse CRP enzyme linked immunosorbent assay kit (ELISA) (Life Diagnostics, West Chester, PA, USA). Serum ALT levels were measured in fed mice using a mouse ALT ELISA kit from BioVision.

2.3.Quantitative Real-Time PCR

Total RNA from liver was extracted using the Tri-Reagent kit (Molecular Research Center, Cincinnati, OH, USA), and gene expression was assessed by quantitative reverse transcription-polymerase chain reaction (PCR) (ABI Universal PCR Master Mix; Thermo Fisher Scientific, Waltham, MA, USA) using a Stratagene Mx3000P thermocycler (Stratagene, La Jolla, CA, USA). The gene expression data were normalized to the house keeping gene 18s. The primer and probe sets used in the assays were purchased from Thermo Fisher Scientific (Waltham, MA, USA) and are further described in **Table 2**.

Table 2 RT-PCR probes ID and sequences

Table 2. RT-PCR probes ID and sequences			
ABI assay ID			
TGFβ1	Mm01178820_m1		
Coll1α1	Mm00801666_g1		
Coll1α2	Mm00483888_m1		
Coll4α1	Mm01210125_m1		
PAI-1	Mm00435860_m1		
IL-6	Mm00446190_m1		
IL-1β	Mm01336189_m1		
TNFα	Mm00443258_m1		
MCP1 (ccl2)	Mm00441242_m1		
FAS	Mm01204974_m1		
SCD1	Mm00772290_m1		
	Forward	Reverse	Probe
18S	AGTCCCTGCCCTTTGTACACA	GATCCGAGGGCCTCACTAAAC	CGCCCGTCGCTACTACCGATTGG
PPAR α	GACAAGGCCTCAGGGTACCA	GCCGAATAGTTCGCCGAAA	AGCCCTTACAGCCTTCACATGCGTGA
Abbreviations: ABI, Applied Biosystems Inc (Foster City, CA , USA); RT-PCR , reverse transcription polymerase chain reaction; FAS, fatty acid synthase; SCD1, stearyl-CoA desaturase-1; COX1, cyclooxygenase 1; AC OX1, acyl-CoA oxidase; CPT1A, carnitine palmitoyltransferase 1A; CPT1B, carnitine palmitoyltransferase 1B; IL -6, interleukin 6; IL -1β, interleukin-1 beta; TNFα, tumor necrosis factor alpha; MCP1, monocyte chemotactic protein 1; ACC , acetyl CoA carboxylase; PPAR α, peroxisome proliferator-activated receptor alpha.			

2.4. Tissue Preparation and Historical Examination

Liver tissues were fixed in 10% neutral formalin, embedded in paraffin, and cut into 5 μm sections. Sections were processed for hematoxylin and eosin staining. For inflammation immunostaining, slides were immunoblotted with CD68 (Bio-Rad MCA 1957) as primary antibody and Biotin-SP-AffiniPure Mouse Anti-Rat IgG as secondary antibody. This was followed by the application of the immunoperoxidase technique with a Vector kit. Areas of staining were quantified with ImageJ and expressed as percentages of the field area. For fibrosis Picro-Sirius Red staining, liver slides were dewaxed and hydrated. Weigert's hematoxylin stained for 8 mins and Picro-Sirius Red (Picro Sirius Red Stain Kit, abcam150681) stained for one hour. Acidified water wash was applied. Slides were dehydrated in three changes of 100% ethanol and Clear in xy-

lene and mounted in a resinous medium. All of the histological images were recorded using Nikon Eclipse E800 Microscopy with Zeiss AxioCam camera in Image Core facility of Georgia State University.

2.5. Hepatic Lipid Analysis

Liver lipid extraction was conducted as previously described by Bligh and Dyer with minor modifications⁴⁶. Briefly, ~100mg of liver was thawed, minced and weighted in glass tube. Add 3ml CHCl₃:MeOH (2:1) to extract lipid at room temperature overnight. Transfer lipid extraction into new glass tube, wash liver tissue with CHCl₃:MeOH (2:1) twice and dry down the combined solvent at 60°C. Add 3ml CHCl₃:MeOH (2:1) and 0.6ml 0.05% H₂SO₄ into tube, and split the phase by 2000rpm centrifugation for 15 minutes. An aliquot of the bottom phase was dried down and the lipid extraction was dissolved in 2% Triton X-100. Triglyceride (TG) was measured using TC, TG kit (Wako Chemicals, USA) with liver weight correction.

2.6. Western Blot

The P-AMPK and AMPK antibodies were obtained from Cell Signaling (Danvers, MA). GAPDH antibody was obtained from Santa Cruz Biotechnology (Santa Cruz, CA). Protein levels of cell extracts were measured by BCA kit (Thermo Scientific). For Western blot, 10-50 µg protein was resolved on 4-15% gradient polyacrylamide gels (Criterion precast gel, Bio-Rad Laboratories, Hercules, CA), transferred to either PVDF or nitrocellulose membranes, incubated in blocking buffer (3% BSA or 5% non-fat dry milk in TBS) and then incubated with primary antibody (1:500 dilution), washed and incubated with horseradish peroxidase- or fluorescence-conjugated secondary antibody (1:5000 dilution). Total ACC was detected using Streptavidin-conjugated horseradish peroxidase (Amersham Biosciences, Piscataway, NJ). Visualization was conducted using BioRad ChemiDoc instrumentation and software (Bio-Rad Laboratories, Hercu-

les, CA) or Li-COR Odyssey Fc Imaging system (Li-COR Biosciences) and band intensity was assessed using Image Lab 4.0 or Quantity One (Bio-Rad Laboratories, Hercules, CA), with correction for background and loading controls

2.7. Statistical Analysis

All data are expressed as mean \pm SEM. Data were analyzed by one-way ANOVA, and significantly different group means ($p < 0.05$) were separated by the least significant difference test using GraphPad Prism version 6 (GraphPad Software, La Jolla California USA, www.graphpad.com).

3. RESULTS

3.1. Leu-Met-Sil combination did not change body weight but decreased liver weight.

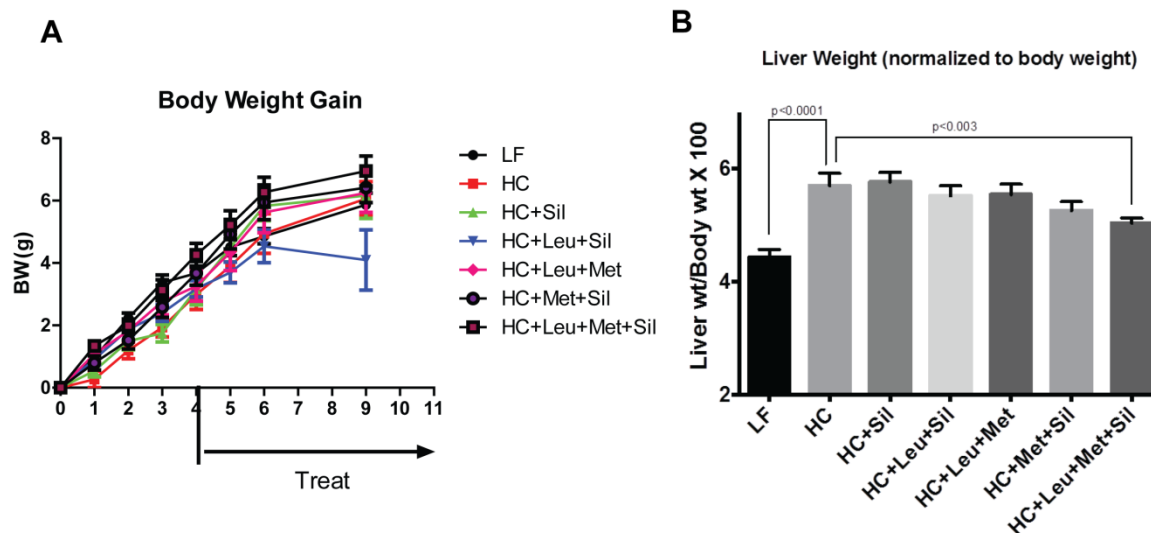


Figure 2. Leu-Met-Sil combination did not change Body weight but changed liver weight.

6-week-old male C57BL/6J mice were put on either a low fat (LF) diet or a HF/atherogenic diet (HF/ATH) containing 1.25% cholesterol by weight and 60% calories as saturated fat (lard) for 4 weeks to induce the development of NASH. The mice were then randomly assigned to receive either the LF or the HF/ATH diet with or without different leucine-metformin-sildenafil combinations indicated below for an additional 5 weeks to study the effect of the treatments on the reversal of NASH. Leucine, metformin and sildenafil were administered via diet. Body weight was measured every week and liver tissue weight was weighed when dissecting the mice. (A) Body weight gain before and after treatment; (B) Liver weight normalized to body weight. The values represent the means \pm SEM. * $P < 0.05$ and ** $P < 0.01$ versus the control group.

Figure 2 Leu-Met-Sil combination did not change body weight but decreased liver weight

To date, NASH studies have been impeded by the absence of a suitable experimental model. Genetic targeted defects²³ and overexpression²⁴ rats have been used in NAFLD model. However, genetic manipulations cannot reflect the natural etiology of NAFLD in clinical studies and rarely lead to the pathology of NASH. The alternative option is nutritional manipulation models. Sucrose-rich and fat-rich diet²⁵ just accumulate minimal fat and develop subtle inflammation in liver. The methionine and choline-deficient model (MCD)^{26, 27} is frequently used to produce more progressive liver pathology. However, this model has no insulin resistance²⁸. In this study, we mainly focus on an atherogenic (Ath) diet, which contains cholesterol and cholic acid. This diet has been reported to induce liver steatosis, inflammation, and fibrosis²⁹

To build the NASH mouse model, eighty 6-week old male C57BL/6 mice from Jackson Lab were put on either a low-fat (LF) diet or a HF/ATH (atherogenesis)(containing 1.25% cholesterol, 0.5% cholate by weight and 60% calories as saturated fat (lard)) for 4 weeks to induce NASH (**Figure 2-A**). To assess the NASH development, blood was collected from tail vein. ELISA method was used to measure alanine aminotransferase (ALT) in serum to detect the liver damage levels. Based on the measured ALT levels, mice were then be assigned to receive either the LF or the HF/ATH diet with or without different Leu-Met-Sil combinations indicated below for an additional 5 weeks (**Figure 2-A**).

Interventions:

LF (10% calories from fat) (**LF** group)

HF/ATH (1.25% cholesterol, 0.5% cholate, 60% calories from fat) (**HC** group)

HF/ATH + leucine (24 g/kg diet) + metformin (0.25 g/kg diet) (**HC+Leu+Met** group)

HF/ATH + Sildenafil (25mg/kg diet) (**HC +Sil** group)

HF/ATH + leucine (24 g/kg diet) + Sildenafil (25mg/kg diet) (**HC+Leu+Sil** group)

HF/ATH + metformin (0.25 g/kg diet) + Sildenafil (25mg/kg diet) (**HC+Met+Sil** group)

HF/ATH + leucine (24 g/kg diet) + metformin (0.25 g/kg diet) + Sildenafil (25mg/kg diet)
(**HC+Leu+Met+Sil** group)

To evaluate the treatment effect, body weight was monitored weekly. Our data (**Figure 2-A**) indicate that there were no changes in body weight among different groups. At the end of the study, the mice were euthanized and liver tissue was dissected. Our data show that Leu-Met-Sil treatment decreased liver weight (normalized to body weight) (**Figure 2. B**).

3.2. Leu-Met-Sil combination reduced ALT levels in serum.

ALT is a liver damage marker, which synthesized by liver and released into circulation when liver is damaged. To study the treatment effects, ALT levels in the serum were measured during treatment. Our data (**Figure 3.A,B**) show that the Leu-Met-Sil combination decreased ALT levels in serum.

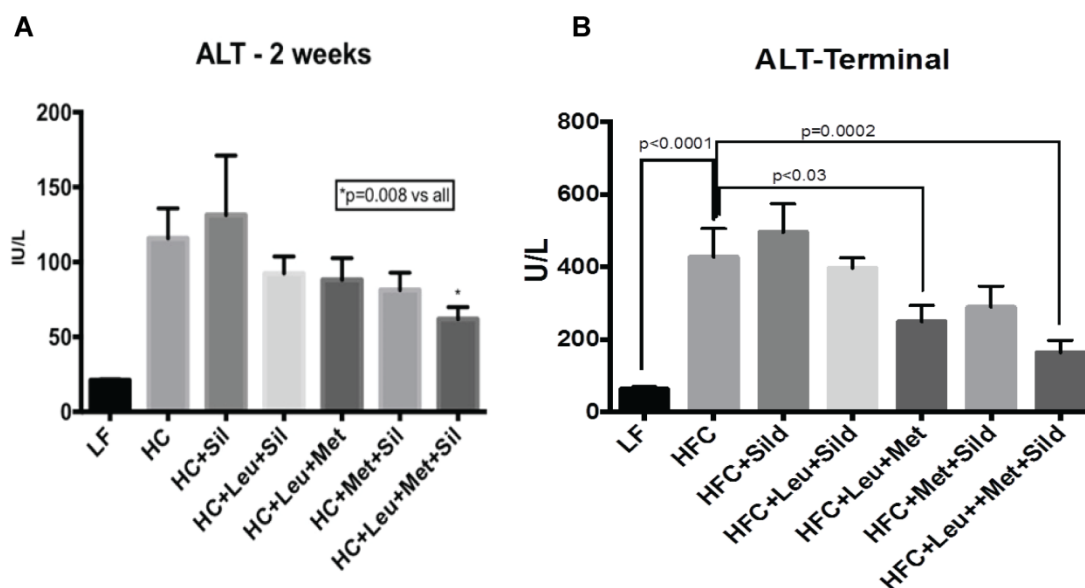


Figure 3. Leu-Met-Sil combination decreased serum ALT levels. Blood was collected from tail vein and centrifuged. Serum was kept at -20°C , and ALT kit from Bivision was used to detect the concentration of ALT in Serum. (A) ALT levels at two weeks after treatment. (C) ALT levels after treatment. ALT, Alanine Aminotransferase; The values represent the means + SEM. *P 0.05 and **P 0.01 versus the control group.

Figure 3 Leu-Met-Sil combination reduced ALT levels in serum.

3.3. Leu-Met-Sil combination reduced liver steatosis and lipid accumulation.

To further evaluate the treatment of the Leu-Met-Sil combination on NASH, Hematoxylin and Eosin staining (H&E staining) was performed in liver tissue to evaluate liver steatosis status. Liver lipids were also extracted and measured. Our data (**Figure 4.A,B**) indicate that Leu-Met-Sil combination decreased liver steatosis and lipid accumulation.

A

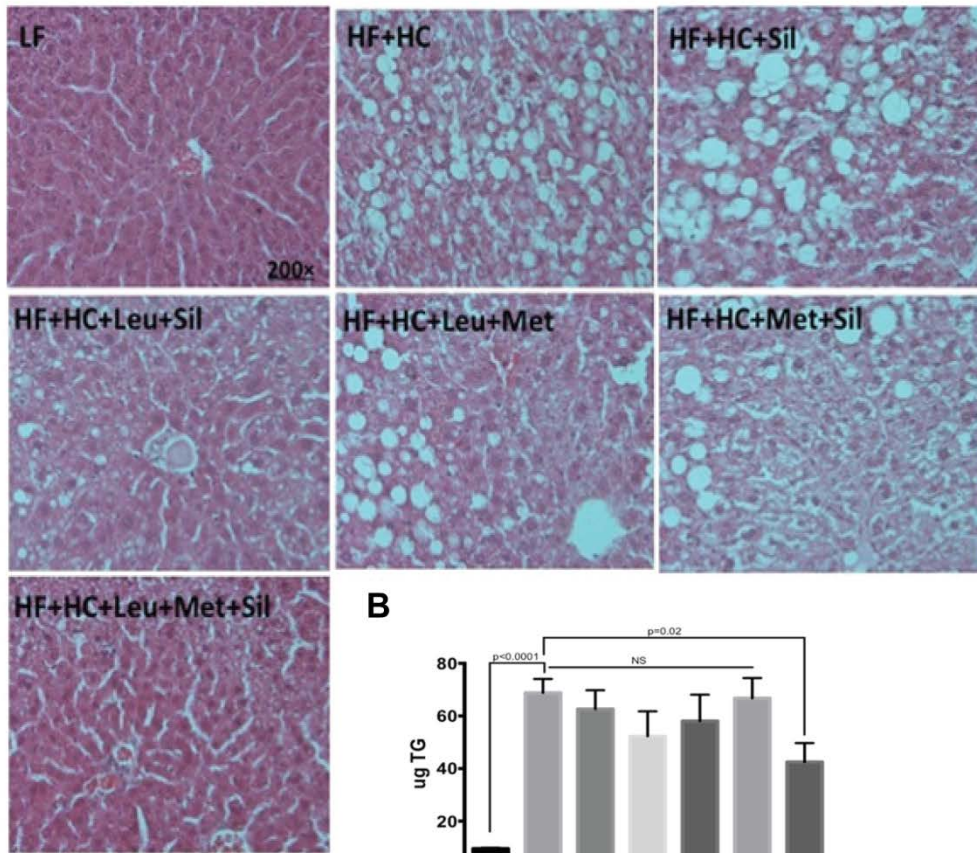


Figure 4. Leu-Met-Sil combination reduced liver steatosis. Liver tissue were collected, formalin fixed, paraffin embedded, and sliced using microtome. The slices were stained using Hematoxilin & Eosin (H&E) method. Liver lipid were extracted from frozen liver tissue. Triglycerides(TG) were measured using the kit (Wako;Japan). (A) H&E staining of liver tissue of different groups (B) Liver TG levels. The values represent the means + SEM. *P 0.05 and **P 0.01 versus the control group.

Figure 4 Leu-Met-Sil combination reduced liver steatosis.

3.4. Leu-Met-Sil combination decreased liver fibrosis.

To assess the effect of Leu-Met-Sil combination on fibrosis, genes involved in fibrosis (Procollagen type I alpha 1 (Col 1a1); procollagen type I alpha 2 (Col 1a2); procollagen type IV alpha 1 (Col 4a1); PAI-1, Plasminogen activator inhibitor 1 (PAI-1)) and Transforming growth factor β (TGF- β) expression of liver were measured using Quantitative polymerase chain reac-

tion (Q-PCR). Our data (**Figure. 5**) show that Leu-Met-Sil combination reduced fibrogenesis gene expression.

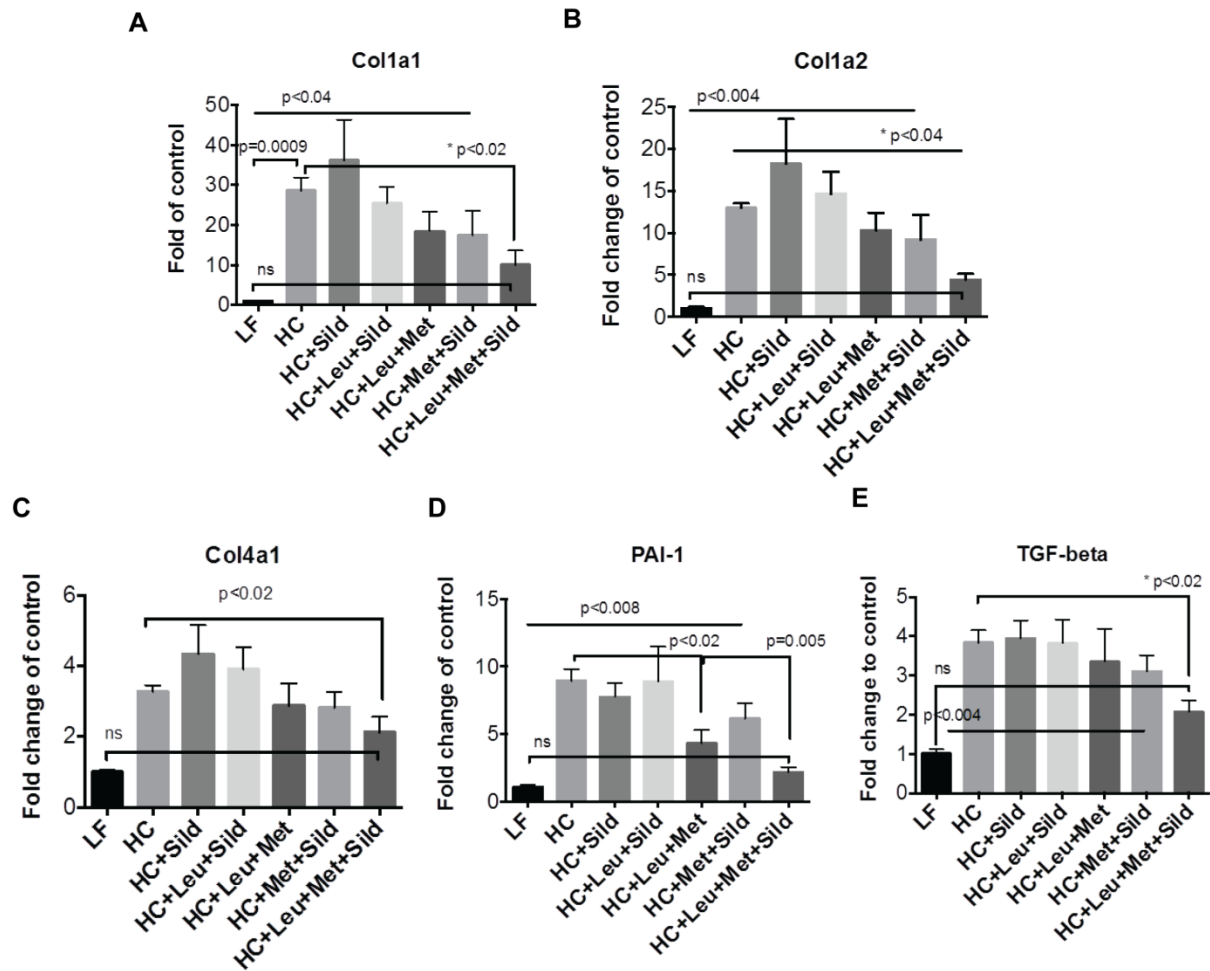


Figure 5. Leu-Met-Sil combination reduced liver fibrogenesis gene expression.

mRNA levels of genes for procollagen type I alpha 1 (Coll1a1), procollagen type I alpha 2 (Coll1a2), procollagen type IV alpha 1 (Coll4a1), plasminogen activator inhibitor 1 (PAI-1), transforming growth factor beta (TGF-beta) in the livers of mice fed on different diet were quantified with real-time PCR. The gene expression was normalized with eukaryotic 18S ribosomal RNA. (**A,B,C,D,E**). Fibrogenesis gene expression. The values represent the means + SEM. *P 0.05 and **P 0.01 versus the control group (HC group).

Figure 5 Leu-Met-Sil combination decreased liver fibrogenesis gene expression.

To more thoroughly evaluate the liver fibrosis, Picro-Sirius Red staining was performed to assess the collagen accumulation. Our results show that (**Figure. 6**) Leu-Met-Sil combination

significantly reduced liver fibrosis.

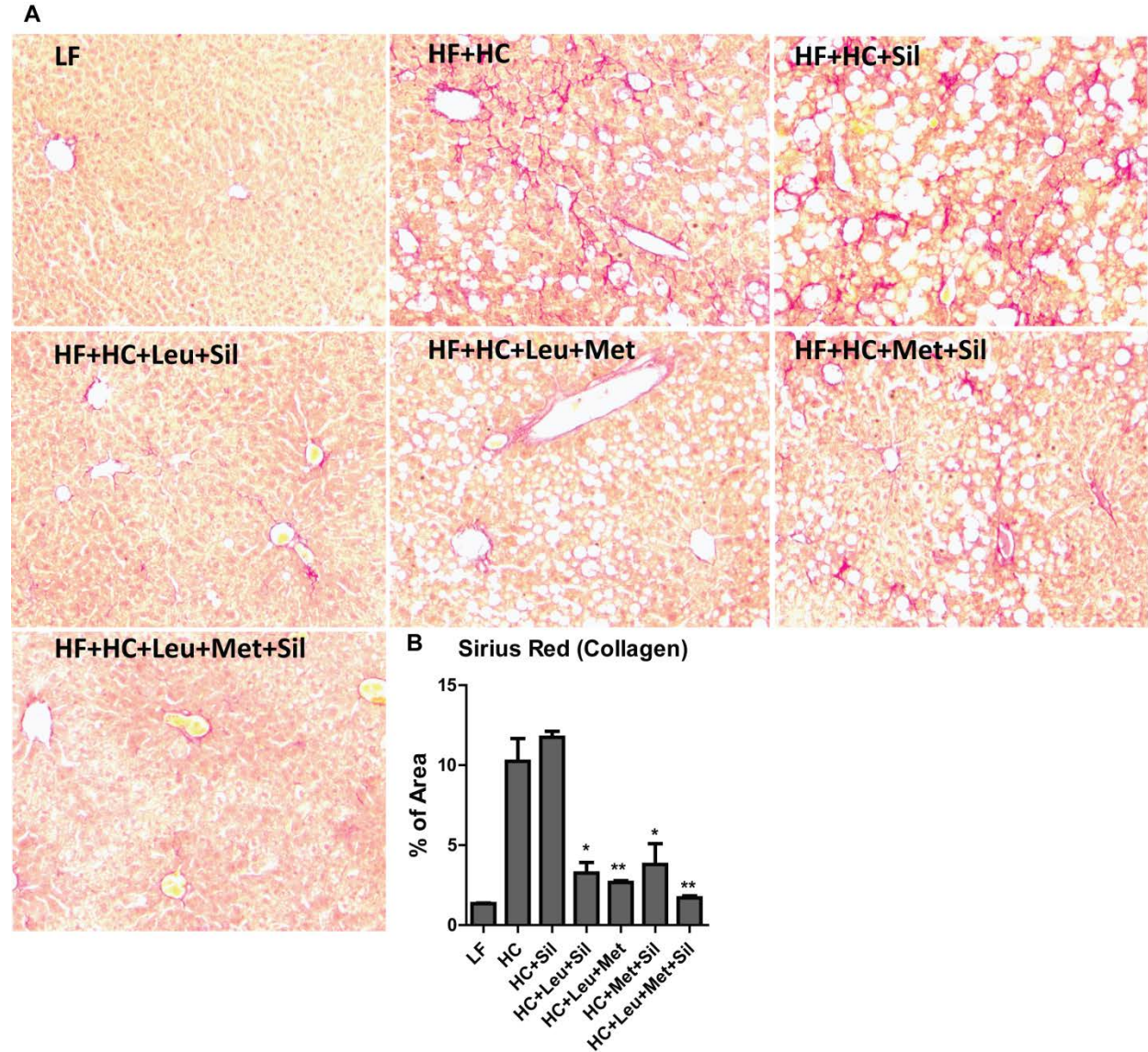


Figure 6. Leu-Met-Sil combination reduced liver fibrosis. Formalin-fixed, paraffin-embedded liver tissue were sliced and stained using Picro Sirius Red Stain Kit (Connective Tissue Stain) (ab150681). (A) Liver Picro-Sirius staining. (B) Quantitation of staining. The values represent the means + SEM. *P 0.05 and **P 0.01 versus the control group

Figure 6 Leu-Met-Sil combination reduced liver fibrosis.

3.5. Leu-Met-Sil combination decreased hepatic inflammation.

To test inflammatory status after Leu-Met-Sil treatment, mRNA was isolated from liver tissue. Pro-inflammatory makers (IL6, IL- β , TNF α , MCP-1) were measured by using Q-PCR. CRP levels in serum were measured using ELISA kit.

Our results indicate that Leu-Met-Sil combination reduced liver pro-inflammatory genes expression (**Figure.7A-D**) and serum C-reaction protein (CRP) levels(**Figure.7E**)

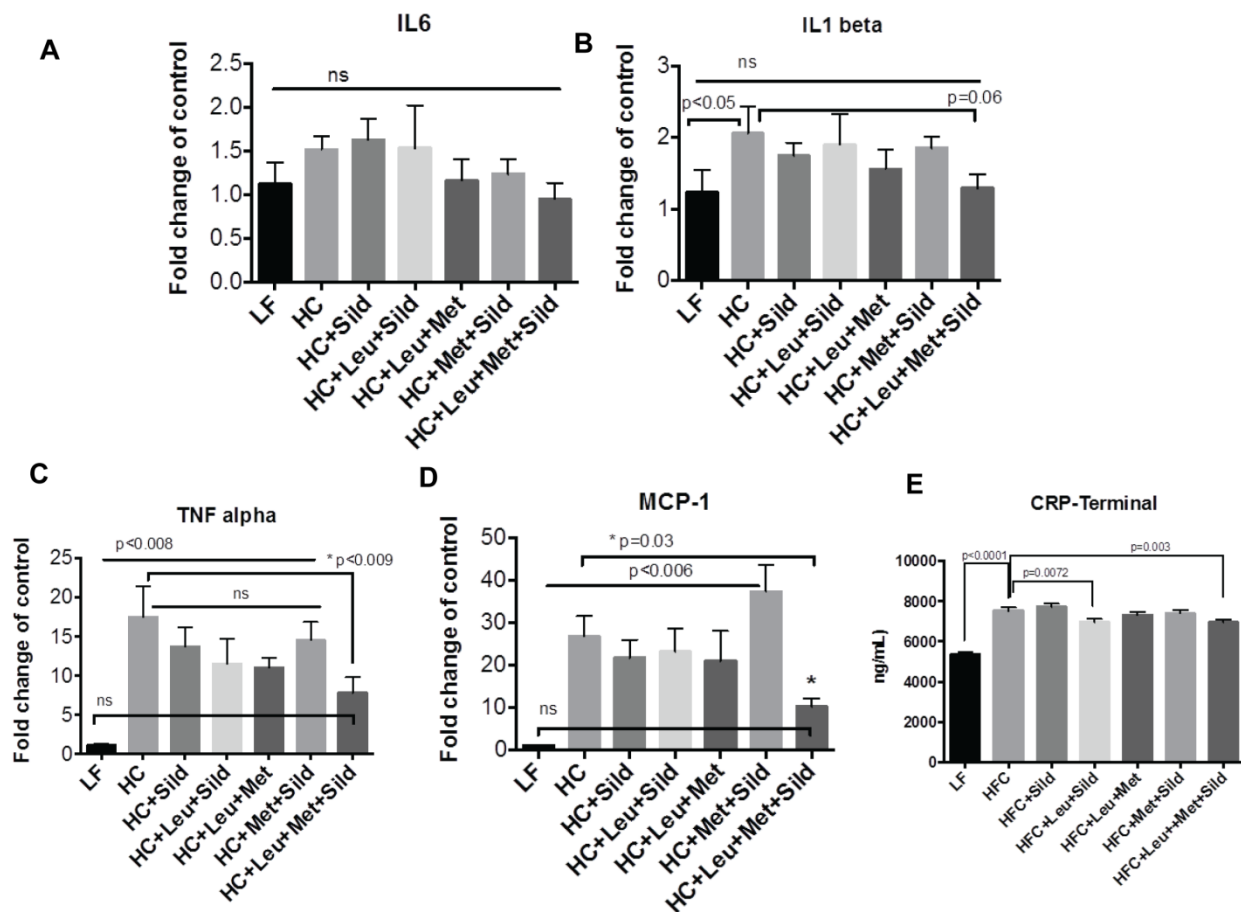


Figure 7. Leu-Met-Sil combination reduced liver proinflammatory gene expression and serum CRP level. Liver tissue were collected. RNA were extracted and Q-PCR was performed to detect the gene expression. Blood was collected when sacrificing the mice and serum was used to detect the CRP levels. **(A-D)** Inflammation gene expression. **(E)** CRP level in serum. CRP, C-reactive Protein, The values represent the means + SEM. *P 0.05 and **P 0.01 versus the control group.

Figure 7 Leu-Met-Sil combination decreased liver proinflammatory gene expression and serum CRP levels.

3.6. Leu-Met-Sil combination decreased liver macrophage infiltration.

To more thoroughly assess liver inflammatory levels, we performed CD68 immunostaining to detect macrophage infiltration. Our data indicate that Leu-Met-Sil combination decreased macrophage infiltration (**Figure. 8**), which further confirmed the anti-inflammatory effect of Leu-Met-Sil combination.

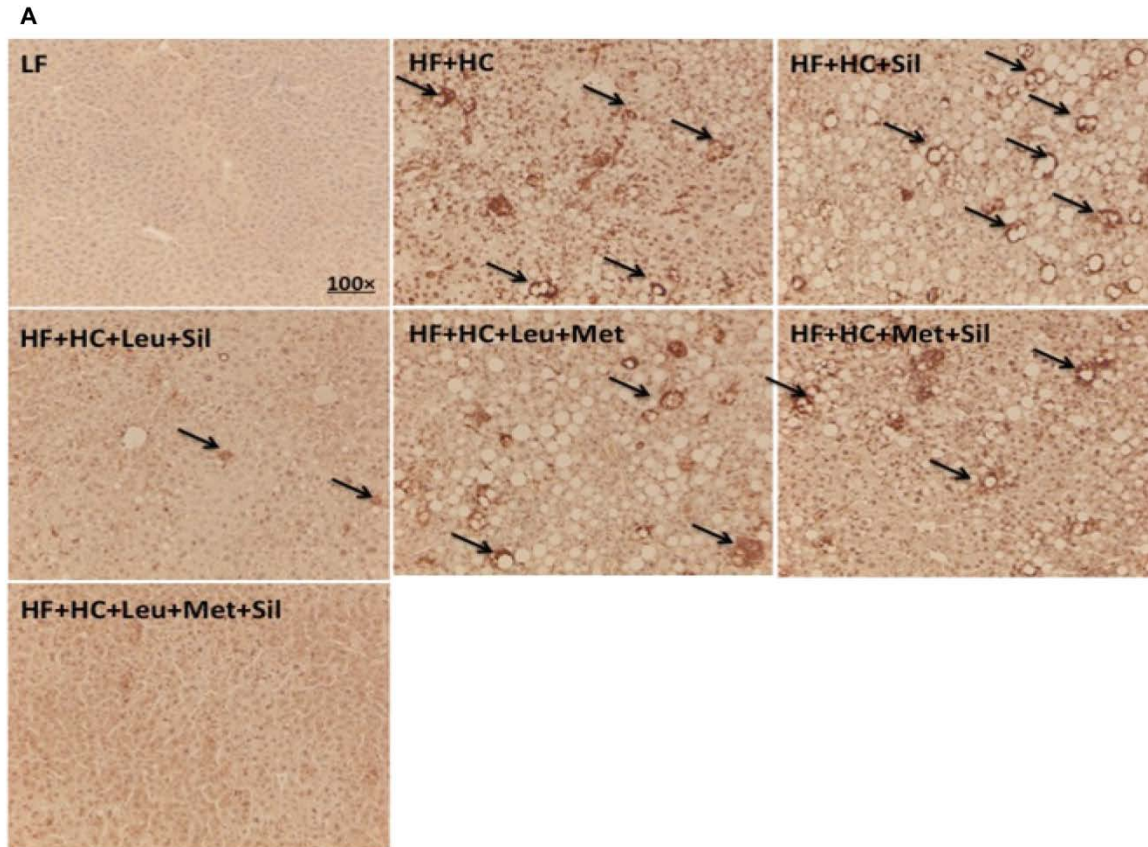


Figure 8. Leu-Met-Sil combined treatment decreases liver macrophage infiltration. Liver were collected, formalin-fixed, paraffin-embed and sliced by microtome. Liver slides were stained using immunohistochemical (IHC) method. **(A)** CD68 immunohistochemical stain in liver of different groups, brown dots are positive staining. The values represent the means + SEM. *P 0.05 and **P 0.01 versus the control group.

Figure 8 Leu-Met-Sil combination decreased liver macrophage infiltration.

3.7. Leu-Met-Sil combination increased the expression of genes involved in fatty acid oxidation in liver.

One of the hallmarks of NASH is lipid accumulation, which is due to dysregulation of fatty acid metabolism, including lipogenesis and fatty acid oxidation.

To examine the status of fatty acid synthesis and oxidation in the liver, we measured the expression of fatty acid synthase (FAS), stearoyl-CoA desaturase 1(SCD1) (**Figure. 9A**) and peroxisome proliferator-activated receptor α (PPAR α) (**Figure. 9B**).

Our data indicate that Leu-Met-Sil combination had a tendency to reduce the expression of SCD1 ($p=0.06$), while significantly upregulating the expression of PPAR α .

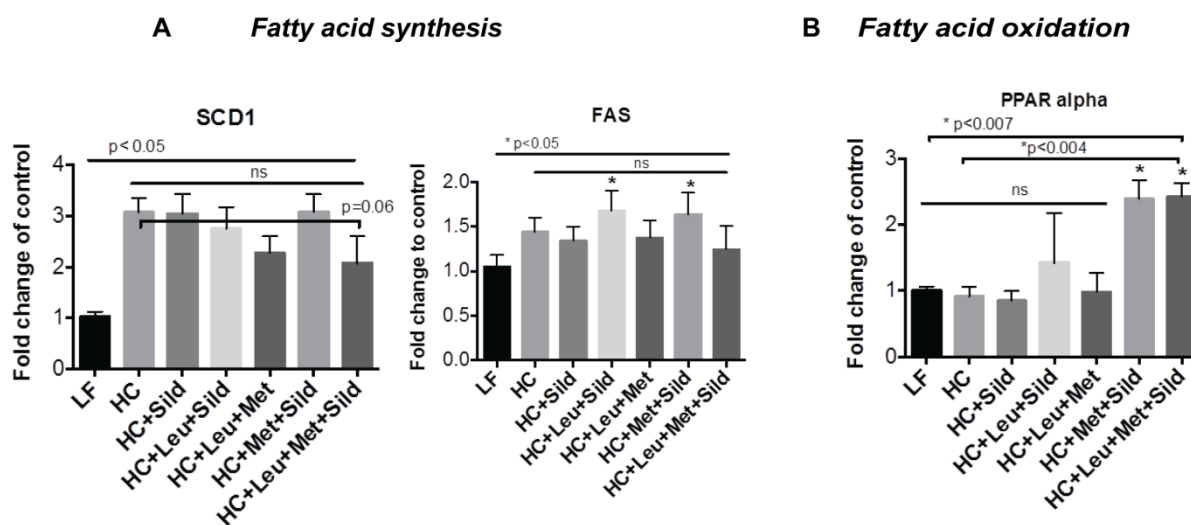


Figure 9 . Leu-Met-Sil combination increased liver fatty acid oxidation representative gene expression. Then mRNA levels of genes for SREBP-1c, SCD-1, FAS, PPAR-alpha, CPT-1a in the livers of mice fed on different diet were quantified with real-time PCR. The gene expression was normalized with eukaryotic 18S ribosomal RNA. (A). Representative gene expression of fatty acid synthesis. (B). Representative gene expression of fatty acid oxidation. The values represent the means + SEM. *P 0.05 and **P 0.01 versus the control group (HC group).

Figure 9. Leu-Met-Sil combination increased the expression of genes involved in hepatic fatty acid oxidation.

3.8. Leu-Met-Sil combination did not change hepatic AMPK signaling.

To investigate whether AMPK mediates the beneficial effect of Leu-Met-Sil combination, we measured phosphorylation of AMPK and its downstream target acetyl-CoA carboxylase (ACC).

Our data show that Leu-Met-Sil combination did not change AMPK signaling (**Figure. 10**), suggesting that Leu-Met-Sil did not function through AMPK pathway.

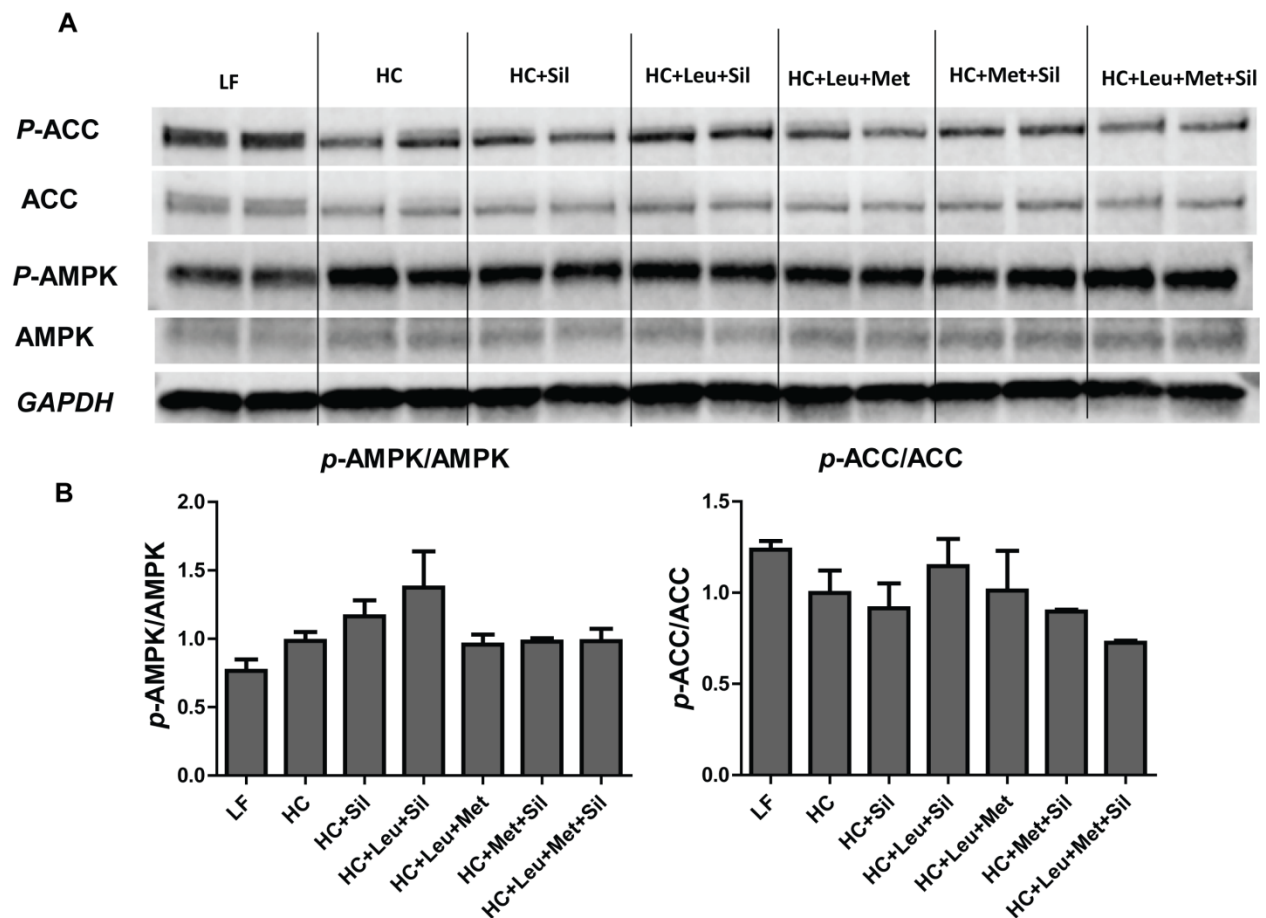


Figure 10. Leu-Met-Sil combination did not change AMPK pathway activity. Liver tissue were collected and protein was extracted. Immunoblotting was performed to detect the protein involved in AMPK pathway. (A) p-AMPK, AMPK, p-ACC, ACC protein expression. (B) Quantitation of immunoblotting. AMPK, AMP protein kinase K; ACC, Acetyl-Coa carboxylase; The values represent the means + SEM. *P 0.05 and **P 0.01 versus the control group (HC group).

Figure 10 Leu-Met-Sil combination did not change hepatic AMPK signaling.

4 DISCUSSION AND CONCLUSION

In this study, our data indicate that leucine-metformin-PDE5i combination reduced serum ALT levels, improved steatosis and hepatic ballooning, decreased inflammation and fibrogenesis representative gene expression, and increased fatty acid oxidation.

NASH is defined as the presence of hepatic steatosis and inflammation with hepatocyte injury (ballooning) with or without fibrosis. To date, there is no efficient management of patient with NASH. Many studies indicate that lifestyle modification may improve hepatic steatosis⁴⁷. In addition, metformin, Thiazolidinediones(TZD) and vitamin E are also used for clinical trials for treating NASH. However, there are either no significant effect or no well-evaluated safety and efficacy in NASH patient. Thus, we investigated the synergistic effect of Leucine, Metformin and PDE5i on NASH.

PDE5-inhibitors, including sildenafil and tadalafil, have been demonstrated to increase SIRT1 signaling in mice,^{30,31} to increase energy expenditure in skeletal muscle cells,⁴⁸ to improve energy balance, and to increase insulin action in both diet-induced obese (DIO), insulin-resistant mice and diabetic patients.^{32, 49} This may be, in part, due to stimulation of eNOS and NO signaling and subsequent NO-mediated SIRT1 activation.^{30,32} Leucine activation of SIRT1 results in downstream activation of AMPK, while metformin activation of AMPK leads to SIRT1 activation via phosphorylation of NAMPT to regenerate NAD⁺. Both AMPK and SIRT1, in turn, activate eNOS via phosphorylation and deacetylation, respectively. The increased NO, in turn, may stimulate SIRT1 activity, resulting in a three-component feed-forward loop.

Inflammation often represents the “second hit” and potentiates the risk for progression from simple steatohepatosis to NASH and cirrhosis.⁵⁰ Obesity is associated with a generalized chronic inflammatory state and pro-inflammatory cytokines such as TNF- α , IL-6 and C-reactive

protein (CRP) are elevated in obese patients.⁵¹ Pro-inflammatory cytokines have been suggested by some as noninvasive biomarkers to distinguish hepatosteatosis from NASH; although the clinical utility of these markers in predicting severity of NASH and fibrosis is unclear, most studies have shown a positive correlation with higher inflammatory marker levels in NASH^{52, 53}. In this study, all of the inflammatory markers in liver (IL6, IL1 beta, TNF alpha and MCP-1) and in plasma (CRP) were significantly blunted by the Let-Met-Silt treatment combinations.

The full therapeutic dose of metformin used in mouse is 300mg/Kg bodyweight (BW) and very low dose is 50mg/Kg BW^{54, 55}. In our study, the intervention dose of metformin is 0.25 g/kg diet (equal to 250mg/Kg diet)¹⁹, which is 25mg/KG BW after converting. Our preliminary data show that this dose of metformin synergized with leucine (24g/Kg diet) had effects against NAFL. The normal leucine dietary intake in diet for a mouse is 60-70 mg/day. However, this dose is sufficient to activate Sirt1 pathway. To achieve this goal, extra leucine is usually administered via water in mouse study and the dose is 1.5g/100ml (1.5% w/v)^{56, 57}. This increases total intake of leucine to 130 mg/day/mouse, which is sufficient to activate Sirt1 pathway⁵⁷. In our experiment, we administered leucine via diet with the dose of 24g/Kg diet, which is 2.4g/Kg BW after converting. This administration can activate Sirt1 activity and make synergy of Leu-Met-Sil become possible.

Now, the absence of experimental model hampered NASH study. Genetic manipulations can evaluate the specific gene importance. However, they might not directly reflect the etiology in human NAFLD and rarely lead us to know the NASH pathology. Nutritional manipulations induced either mild NASH such as sucrose-rich and fat-rich diet or more progressive liver damage such as methionine and choline deficient (MCD) model. In this study, we use ATH diet induced NASH, which is a more physiological model compared with the models above. No genetic

or nutrient deficiency is involved in this model. Cholesterol and cholate are the main ingredients in the diet. These components resulted in accumulated cholesterol in the liver and induced steatosis by cholesterol-induced toxicity. However, this model has some limitations, because it is still controversial that whether cholesterol, TG, FFA contributes to the development of NASH. In addition, it is not a well-studied NASH model. The exact molecular mechanisms involved in this model are still unknown. In our results, we just observed the phenotype changes before and after the combination. However, the real reason why Leu-Met-Sil combination has effects is still unknown. In the future study, we might use a different NASH model to study the development of NASH.

In this study, Leu-Met-Sil combination did not significantly change fatty acid synthesis representative genes. Furthermore, AMPK is not involved in synergistic effects of Leu-Met-Sil. Leu-Met-Sil combination increased PPAR- α expression and decreased liver inflammation levels, which is a good explanation of decreased fibrosis. Other downstream pathways of PPAR-alpha might involve in the combination effect, such as fatty acid transport protein (FATP), fatty acid translocase (FAT). The synergistic effects of Leu-Met-Sil might converge on the PDE5 inhibitor pathway. They might enhance cGMP-dependent protein kinases (PKG) activity and then decrease liver inflammation and fibrosis⁵⁸⁻⁶⁰.

In summary, Leu-Met-Sil combination improves NASH in Ath-induced NASH model and may give us a potential therapy for NASH in the future.

REFERENCES

1. Brunt, E.M. Nonalcoholic steatohepatitis: definition and pathology. *Semin Liver Dis* **21**, 3-16 (2001).
2. Caldwell, S.H. et al. Cryptogenic cirrhosis: clinical characterization and risk factors for underlying disease. *Hepatology* **29**, 664-9 (1999).
3. Boyle, J.P. et al. Projection of diabetes burden through 2050: impact of changing demography and disease prevalence in the U.S. *Diabetes Care* **24**, 1936-40 (2001).
4. James, P.T., Leach, R., Kalamara, E. & Shayeghi, M. The worldwide obesity epidemic. *Obes Res* **9 Suppl 4**, 228S-233S (2001).
5. Sanyal, A.J., Friedman, S.L., McCullough, A.J. & Dimick-Santos, L. Challenges and opportunities in drug and biomarker development for nonalcoholic steatohepatitis: Findings and recommendations from an American Association for the Study of Liver Diseases-U.S. Food and Drug Administration Joint Workshop. *Hepatology* **61**, 1392-405 (2015).
6. Canto, C. & Auwerx, J. PGC-1alpha, SIRT1 and AMPK, an energy sensing network that controls energy expenditure. *Curr Opin Lipidol* **20**, 98-105 (2009).
7. Gomes, A.P. et al. Declining NAD(+) induces a pseudohypoxic state disrupting nuclear-mitochondrial communication during aging. *Cell* **155**, 1624-38 (2013).
8. Price, N.L. et al. SIRT1 is required for AMPK activation and the beneficial effects of resveratrol on mitochondrial function. *Cell Metab* **15**, 675-90 (2012).
9. Gowans, G.J., Hawley, S.A., Ross, F.A. & Hardie, D.G. AMP is a true physiological regulator of AMP-activated protein kinase by both allosteric activation and enhancing net phosphorylation. *Cell Metab* **18**, 556-66 (2013).
10. Jager, S., Handschin, C., St-Pierre, J. & Spiegelman, B.M. AMP-activated protein kinase (AMPK) action in skeletal muscle via direct phosphorylation of PGC-1alpha. *Proc Natl Acad Sci U S A* **104**, 12017-22 (2007).
11. Brenmoehl, J. & Hoeflich, A. Dual control of mitochondrial biogenesis by sirtuin 1 and sirtuin 3. *Mitochondrion* **13**, 755-61 (2013).
12. Coughlan, K.A., Valentine, R.J., Ruderman, N.B. & Saha, A.K. AMPK activation: a therapeutic target for type 2 diabetes? *Diabetes Metab Syndr Obes* **7**, 241-53 (2014).
13. Pfluger, P.T., Herranz, D., Velasco-Miguel, S., Serrano, M. & Tschop, M.H. Sirt1 protects against high-fat diet-induced metabolic damage. *Proc Natl Acad Sci U S A* **105**, 9793-8 (2008).
14. Milne, J.C. et al. Small molecule activators of SIRT1 as therapeutics for the treatment of type 2 diabetes. *Nature* **450**, 712-6 (2007).
15. Bruckbauer, A. & Zemel, M.B. Synergistic effects of polyphenols and methylxanthines with Leucine on AMPK/Sirtuin-mediated metabolism in muscle cells and adipocytes. *PLoS One* **9**, e89166 (2014).
16. Liang, C., Curry, B.J., Brown, P.L. & Zemel, M.B. Leucine Modulates Mitochondrial Biogenesis and SIRT1-AMPK Signaling in C2C12 Myotubes. *J Nutr Metab* **2014**, 239750 (2014).
17. Bruckbauer, A. et al. Synergistic effects of leucine and resveratrol on insulin sensitivity and fat metabolism in adipocytes and mice. *Nutr Metab (Lond)* **9**, 77 (2012).

18. Bruckbauer, A. & Zemel, M.B. Synergistic effects of metformin, resveratrol, and hydroxymethylbutyrate on insulin sensitivity. *Diabetes Metab Syndr Obes* **6**, 93-102 (2013).
19. Fu, L. et al. Leucine amplifies the effects of metformin on insulin sensitivity and glycemic control in diet-induced obese mice. *Metabolism* **64**, 845-56 (2015).
20. Nisoli, E. et al. Calorie restriction promotes mitochondrial biogenesis by inducing the expression of eNOS. *Science* **310**, 314-7 (2005).
21. Shinmura, K., Tamaki, K. & Bolli, R. Impact of 6-mo caloric restriction on myocardial ischemic tolerance: possible involvement of nitric oxide-dependent increase in nuclear Sirt1. *Am J Physiol Heart Circ Physiol* **295**, H2348-55 (2008).
22. Mattagajasingh, I. et al. SIRT1 promotes endothelium-dependent vascular relaxation by activating endothelial nitric oxide synthase. *Proc Natl Acad Sci U S A* **104**, 14855-60 (2007).
23. Spallotta, F. et al. A nitric oxide-dependent cross-talk between class I and III histone deacetylases accelerates skin repair. *J Biol Chem* **288**, 11004-12 (2013).
24. Chen, Z.P. et al. AMP-activated protein kinase phosphorylation of endothelial NO synthase. *FEBS Lett* **443**, 285-9 (1999).
25. Zhang, Y. et al. AMP-activated protein kinase is involved in endothelial NO synthase activation in response to shear stress. *Arterioscler Thromb Vasc Biol* **26**, 1281-7 (2006).
26. Francis, S.H., Busch, J.L., Corbin, J.D. & Sibley, D. cGMP-dependent protein kinases and cGMP phosphodiesterases in nitric oxide and cGMP action. *Pharmacol Rev* **62**, 525-63 (2010).
27. Schluesener, J.K. & Schluesener, H. Plant polyphenols in the treatment of age-associated diseases: revealing the pleiotropic effects of icariin by network analysis. *Mol Nutr Food Res* **58**, 49-60 (2014).
28. Musicki, B., Bivalacqua, T.J., Champion, H.C. & Burnett, A.L. Sildenafil promotes eNOS activation and inhibits NADPH oxidase in the transgenic sickle cell mouse penis. *J Sex Med* **11**, 424-30 (2014).
29. Das, A., Xi, L. & Kukreja, R.C. Phosphodiesterase-5 inhibitor sildenafil preconditions adult cardiac myocytes against necrosis and apoptosis. Essential role of nitric oxide signaling. *J Biol Chem* **280**, 12944-55 (2005).
30. Shalwala, M. et al. Sirtuin 1 (SIRT1) activation mediates sildenafil induced delayed cardioprotection against ischemia-reperfusion injury in mice. *PLoS One* **9**, e86977 (2014).
31. Koka, S., Aluri, H.S., Xi, L., Lesnefsky, E.J. & Kukreja, R.C. Chronic inhibition of phosphodiesterase 5 with tadalafil attenuates mitochondrial dysfunction in type 2 diabetic hearts: potential role of NO/SIRT1/PGC-1alpha signaling. *Am J Physiol Heart Circ Physiol* **306**, H1558-68 (2014).
32. Ayala, J.E. et al. Chronic treatment with sildenafil improves energy balance and insulin action in high fat-fed conscious mice. *Diabetes* **56**, 1025-33 (2007).
33. Fu, L. et al. Interaction between leucine and phosphodiesterase 5 inhibition in modulating insulin sensitivity and lipid metabolism. *Diabetes Metab Syndr Obes* **8**, 227-39 (2015).
34. Viollet, B. et al. Cellular and molecular mechanisms of metformin: an overview. *Clin Sci (Lond)* **122**, 253-70 (2012).

35. Garber, A.J., Duncan, T.G., Goodman, A.M., Mills, D.J. & Rohlf, J.L. Efficacy of metformin in type II diabetes: results of a double-blind, placebo-controlled, dose-response trial. *Am J Med* **103**, 491-7 (1997).
36. Pawlyk, A.C., Giacomini, K.M., McKeon, C., Shuldiner, A.R. & Florez, J.C. Metformin pharmacogenomics: current status and future directions. *Diabetes* **63**, 2590-9 (2014).
37. Hundal, R.S. et al. Mechanism by which metformin reduces glucose production in type 2 diabetes. *Diabetes* **49**, 2063-9 (2000).
38. Kristensen, J.M., Treebak, J.T., Schjerling, P., Goodyear, L. & Wojtaszewski, J.F. Two weeks of metformin treatment induces AMPK-dependent enhancement of insulin-stimulated glucose uptake in mouse soleus muscle. *Am J Physiol Endocrinol Metab* **306**, E1099-109 (2014).
39. Fischer, M. et al. Metformin induces glucose uptake in human preadipocyte-derived adipocytes from various fat depots. *Diabetes Obes Metab* **12**, 356-9 (2010).
40. Owen, M.R., Doran, E. & Halestrap, A.P. Evidence that metformin exerts its anti-diabetic effects through inhibition of complex 1 of the mitochondrial respiratory chain. *Biochem J* **348 Pt 3**, 607-14 (2000).
41. Ouyang, J., Parakhia, R.A. & Ochs, R.S. Metformin activates AMP kinase through inhibition of AMP deaminase. *J Biol Chem* **286**, 1-11 (2011).
42. Caton, P.W. et al. Metformin suppresses hepatic gluconeogenesis through induction of SIRT1 and GCN5. *J Endocrinol* **205**, 97-106 (2010).
43. Ruderman, N.B. et al. AMPK and SIRT1: a long-standing partnership? *Am J Physiol Endocrinol Metab* **298**, E751-60 (2010).
44. Ruderman, N.B., Carling, D., Prentki, M. & Cacicedo, J.M. AMPK, insulin resistance, and the metabolic syndrome. *J Clin Invest* **123**, 2764-72 (2013).
45. Sun, C. et al. SIRT1 improves insulin sensitivity under insulin-resistant conditions by repressing PTP1B. *Cell Metab* **6**, 307-19 (2007).
46. Bligh, E.G. & Dyer, W.J. A rapid method of total lipid extraction and purification. *Can J Biochem Physiol* **37**, 911-7 (1959).
47. Ueno, T. et al. Therapeutic effects of restricted diet and exercise in obese patients with fatty liver. *J Hepatol* **27**, 103-7 (1997).
48. Sabatini, S., Sgro, P., Duranti, G., Ceci, R. & Di Luigi, L. Tadalafil alters energy metabolism in C2C12 skeletal muscle cells. *Acta Biochim Pol* **58**, 237-41 (2011).
49. Jansson, P.A. et al. Tadalafil increases muscle capillary recruitment and forearm glucose uptake in women with type 2 diabetes. *Diabetologia* **53**, 2205-8 (2010).
50. Boppidi, H. & Daram, S.R. Nonalcoholic fatty liver disease: hepatic manifestation of obesity and the metabolic syndrome. *Postgrad Med* **120**, E01-7 (2008).
51. Mraz, M. & Haluzik, M. The role of adipose tissue immune cells in obesity and low-grade inflammation. *J Endocrinol* **222**, R113-27 (2014).
52. Pearce, S.G., Thosani, N.C. & Pan, J.J. Noninvasive biomarkers for the diagnosis of steatohepatitis and advanced fibrosis in NAFLD. *Biomark Res* **1**, 7 (2013).
53. Abiru, S. et al. Serum cytokine and soluble cytokine receptor levels in patients with non-alcoholic steatohepatitis. *Liver Int* **26**, 39-45 (2006).
54. Hou, M. et al. Protective effect of metformin in CD1 mice placed on a high carbohydrate-high fat diet. *Biochem Biophys Res Commun* **397**, 537-42 (2010).

55. Souza-Mello, V. et al. Comparative effects of telmisartan, sitagliptin and metformin alone or in combination on obesity, insulin resistance, and liver and pancreas remodelling in C57BL/6 mice fed on a very high-fat diet. *Clin Sci (Lond)* **119**, 239-50 (2010).
56. Li, H., Xu, M., Lee, J., He, C. & Xie, Z. Leucine supplementation increases SIRT1 expression and prevents mitochondrial dysfunction and metabolic disorders in high-fat diet-induced obese mice. *Am J Physiol Endocrinol Metab* **303**, E1234-44 (2012).
57. Macotela, Y. et al. Dietary leucine--an environmental modifier of insulin resistance acting on multiple levels of metabolism. *PLoS One* **6**, e21187 (2011).
58. Handa, P. et al. Reduced vascular nitric oxide-cGMP signaling contributes to adipose tissue inflammation during high-fat feeding. *Arterioscler Thromb Vasc Biol* **31**, 2827-35 (2011).
59. Tateya, S. et al. Endothelial NO/cGMP/VASP signaling attenuates Kupffer cell activation and hepatic insulin resistance induced by high-fat feeding. *Diabetes* **60**, 2792-801 (2011).
60. Rizzo, N.O. et al. Reduced NO-cGMP signaling contributes to vascular inflammation and insulin resistance induced by high-fat feeding. *Arterioscler Thromb Vasc Biol* **30**, 758-65 (2010).

APPENDICES**Appendix A***Appendix A.1**Appendix A.2***Appendix B****Appendix C**